

Preparation and Study of Thermal Properties of Phase Change Materials Based on Paraffin–Alumina-Filled Polyethylene

Amir Reza Vakhshouri, Azizov Akif, Aliyeva Reyhan, Martinova Gala, Quliev Akif

Department of Chemical Sciences, Institute of Petrochemical Processes named after Yu. H. Mamedaliyev, Azerbaijan National Academy of Sciences, Baku, Azerbaijan

Received 22 March 2010; accepted 21 August 2010

DOI 10.1002/app.33268

Published online 7 December 2010 in Wiley Online Library (wileyonlinelibrary.com).

ABSTRACT: Novel phase change materials based on paraffin and alumina-filled polyethylene (FPE) were prepared using a two-step process. In the first step, PE is synthesized using metallocene catalyst system. The synthesized PE is subsequently purified, whereas hydrated alumina–PE composites will be formed by the hydrolysis of aluminum organic cocatalyst and dispersion of hydrated alumina in the PE matrix. In the second step, paraffin–alumina–FPE composites were prepared by using the *ex situ* technique. Scanning electron microscopy, X-ray diffraction, Fourier-transform infrared spectroscopy, thermogravimetric

analysis, and differential scanning calorimetry were used to evaluate the structure and thermal properties of the composites. The results show that the incorporation of a suitable amount of alumina into the composites changes their thermal stability. It is also possible to improve the thermophysical properties of the thermal energy storage materials by altering the paraffin ratio to the FPE. © 2010 Wiley Periodicals, Inc. *J Appl Polym Sci* 120: 1907–1915, 2011

Key words: PE; phase change materials; thermal properties; DSC

INTRODUCTION

In recent years, thermal energy storage technologies are used for solar, thermal, and environmentally friendly heating and cooling systems.^{1–3} There are several types of thermal energy storage, which include sensible heat storage, latent heat storage, and reversible chemical reaction heat storage. Latent heat storage, which is carried out by using phase change materials (PCMs), is the most attractive. The PCMs are able to store and release very large quantities of energy per weight of materials as latent heat of fusion at a constant temperature. There are very extensive applications of the PCMs, such as solar energy systems, central air-conditioning systems, thermal protection of electronic devices, thermal protection of food and medical goods, passive storage in bioclimatic buildings, use of off-peak rates and reduction of installed power, and thermal comfort in vehicles.^{1–7}

Scientists identified a large number of inorganic compounds (such as salt hydrates and metallic), organic compounds (such as paraffin, fatty acids, and esters), and mixtures of the two that act as PCMs. Among the various kinds of PCMs, paraffin is found to exhibit many desirable characteristics. These characteristics include high heat of fusion, varied phase

change temperature, and negligible super cooling. They are also found to be chemically inert and stable, self-nucleating, free from phase segregation, and commercially available at a reasonable cost. The carbon atom chain lengths for paraffin waxes, with a melting temperature between 30°C and 90°C, usually range from 18 to 50 (C18–C50). Increased length of the carbon atom chains increases molecular weight and results in a higher melting temperature of the material. The specific heat capacity of latent-heat paraffin waxes is about 2.1 kJ kg⁻¹ K⁻¹. Their melting enthalpy lies between 180 and 230 kJ kg⁻¹, which is very high for organic materials. The combination of these two values results in an excellent energy storage density.^{4,6–11}

Paraffin waxes blended with polymers, especially polyethylene (PE), seem to be the best candidates for preparation of smart polymeric PCMs. Blending of paraffin waxes with polymers provides an opportunity to use PCMs with a unique controlled structure. A polymeric matrix fixes a PCM in compact form, even after its melting, and suppresses leaching. Such materials are easily shaped, and the polymeric phase provides its own specific properties.¹² However, the lower thermal stability, thermal conductivity, and flammability properties have severely restricted the wide applications, especially in the building fields.¹³ Therefore, studies to improve these characteristics of the PCMs are very important. In this study, we prepared composites, improved these characteristics by a new environmentally friendly method, and studied the structure, thermal characteristic, and behavior of enthalpy at melting points.

Correspondence to: A. R. Vakhshouri (amir.vakhshouri@gmail.com).

EXPERIMENTS

Materials

Paraffin was available as a technical grade white powder with a melting temperature of (T_m) 55–65°C, latent heat of 221.5 kJ kg⁻¹, *N*-alkanes 73.9%, iso + cyclo alkanes 26.1%, and oil content 0.4%. Metallocene type of catalyst components includes Cp₂TiCl₂ from TCI-EP (Chuo-ku, Tokyo, Japan), and AlEt₂Cl and methylaluminoxane (MAO) from Aldrich (St. Louis, MO). Polymerization grade ethylene (EP-300 plant, Sumgait, Azerbaijan) and solvents (*n*-hexane, toluene, and ethanol) from Aldrich (St. Louis, MO) were used.

TABLE I
The Samples Identifications and Composition

Samples	Composition
PFPC1	Paraffin 30 wt % + FPE 70 wt %
PFPC2	Paraffin 20 wt % + FPE 80 wt %
PFPC3	Paraffin 10 wt % + FPE 90 wt %
PFPC4	Paraffin 5 wt % + FPE 95 wt %

Preparation of filled PE by particles of hydrated alumina

PE was synthesized at an ethylene pressure of 8.5–15 atm in a stainless steel reactor with 5 mg Cp₂TiCl₂ as catalyst and 3 mL of AlEt₂Cl (30% in toluene) and 4 mL

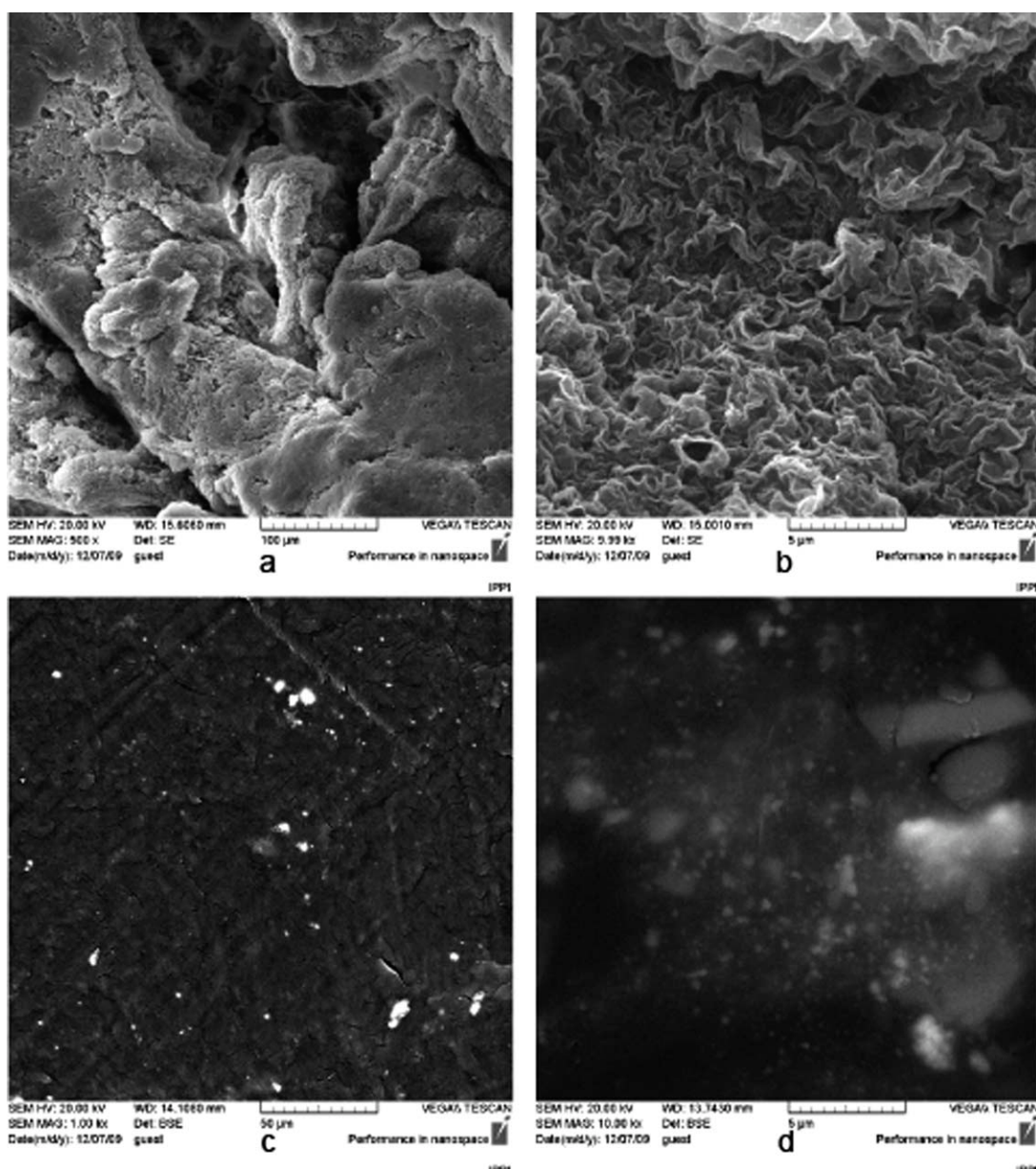


Figure 1 SEM images of the clean PE at $\times 500$ (a) and $\times 10,000$ (b) magnifications, and hydrated alumina-FPE at $\times 1000$ (c) and $\times 10,000$ (d) magnifications.

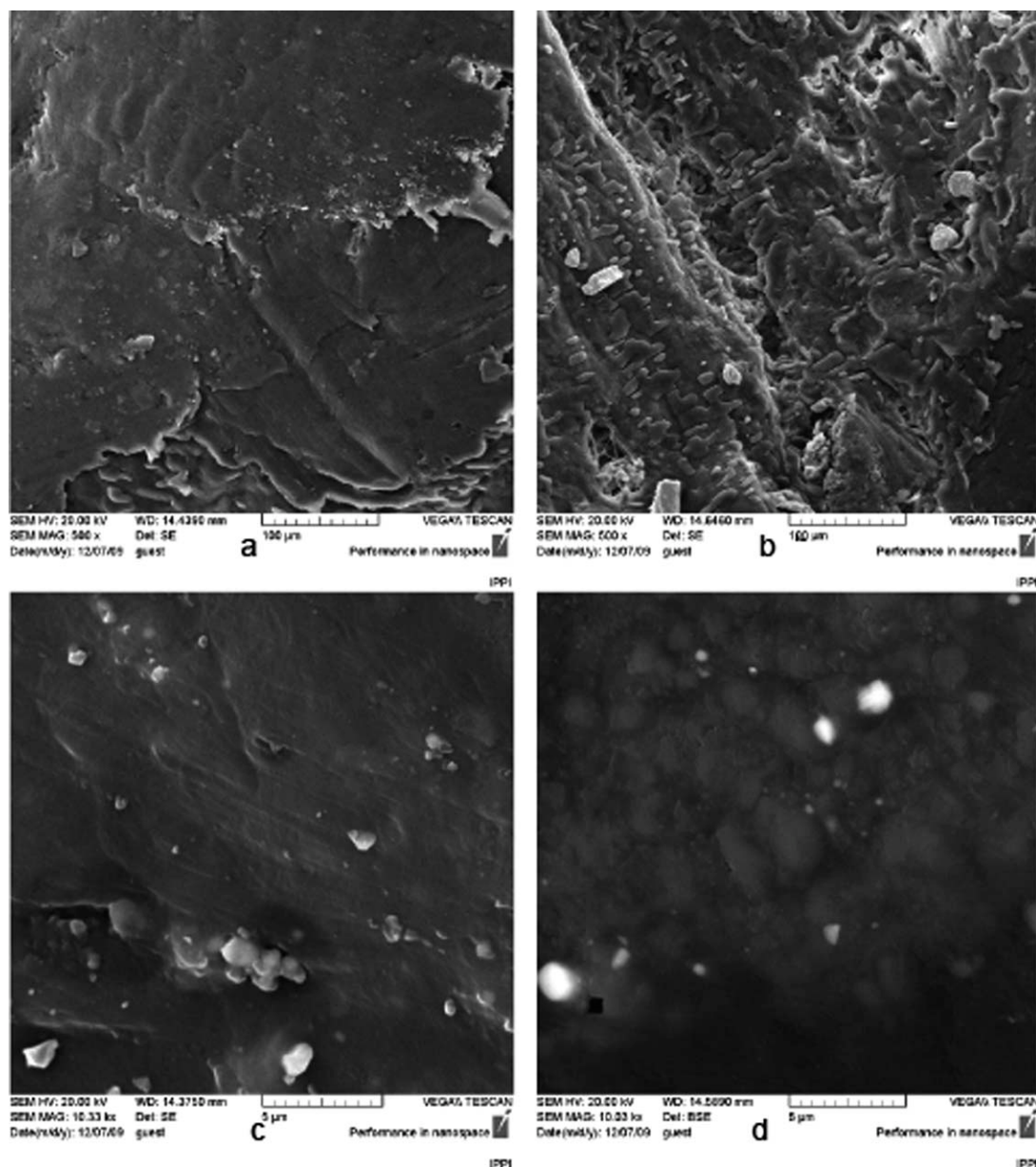
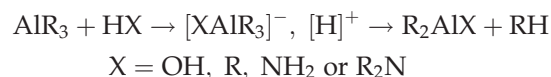


Figure 2 SEM images of PFPC1 at $\times 500$ (a) and $\times 10,000$ (c) magnifications, and PFPC2 at $\times 500$ (b) and $\times 10,000$ (d) magnifications.

MAO (10% in toluene) mixture as cocatalysts. The reaction mixture was stirred at room temperature for 25–30 min. The ratio of Ti/Al was 1/600. The first step of the synthesized PE purification includes washing with 5% hydrochloric acid in ethanol, filtering, and washing with *n*-hexane, but the second step needs a high concentration of hydrochloric acid, ethanol, and large amount of *n*-hexane. By removing this step, the particles of aluminum-containing inorganic compounds, especially hydrated alumina that remained from hydrolyzation of the MAO and AlEt_2Cl , stayed in the PE matrix. The aluminum-containing inorganic compounds' weight was about 10–15% of product.

It is known that the aluminum organic compounds, including MAO, are hydrolyzed as a result of interaction with electron-donor compounds containing an active hydrogen atom (water, alcohol, ammonia, primary and secondary amines, etc.).^{14,15}



Preparation of paraffin–alumina-filled PE composites (PFPCs)

Composites with different weight percentages of paraffin wax (30, 20, 10, and 5) to filled PE (FPE) were

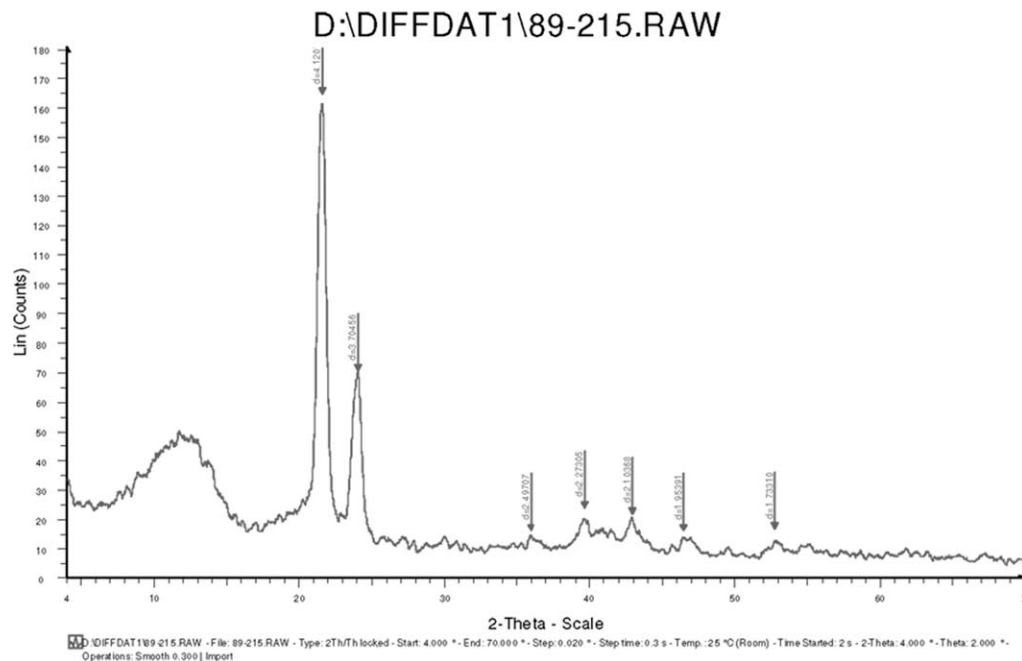


Figure 3 The X-ray diffraction spectra of PFPC1.

prepared (Table I). Paraffin and hydrated alumina-FPE were premixed in a stainless steel bowl. The mixture was then melted at a temperature higher than the melting point of FPE (160°C) in a glycerol bath while stirring with a stainless steel blender, and, subsequently, the composite was cooled to room temperature.

Characterization

Scanning electron microscopy (SEM) was used to characterize the composites morphology. The composites specimens were broken in liquid nitrogen, and the fractured surfaces were coated with gold

before SEM investigations. SEM images were obtained on a S360 SEM microscope.

X-ray diffraction experiments were carried out on the D-5000 (Siemens) instrument. Scattering patterns were obtained with Cu K α radiation (40 kV, 30 mA) at a rate of 2°/min. Fourier transform infrared (FTIR) spectra were obtained using a Bruker Tensor 27 spectrometer for characterization of the composites at room temperature.

Thermogravimetric analyses (TGA) were carried out by using a TGA-PL thermoanalyzer instrument, from 25°C to 650°C with a linear heating rate of 10°C/min

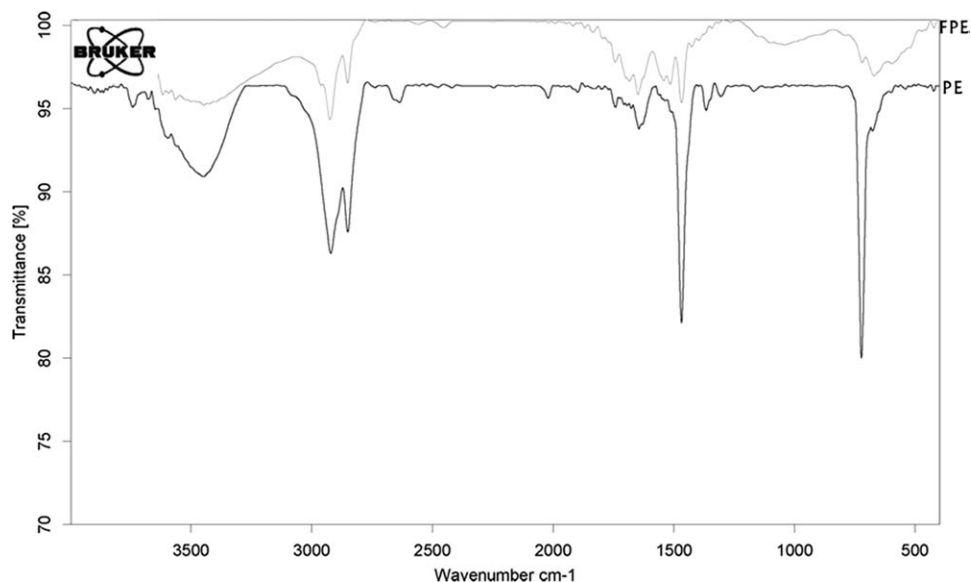


Figure 4 The FTIR spectra of clean PE and FPE by hydrated Al₂O₃.

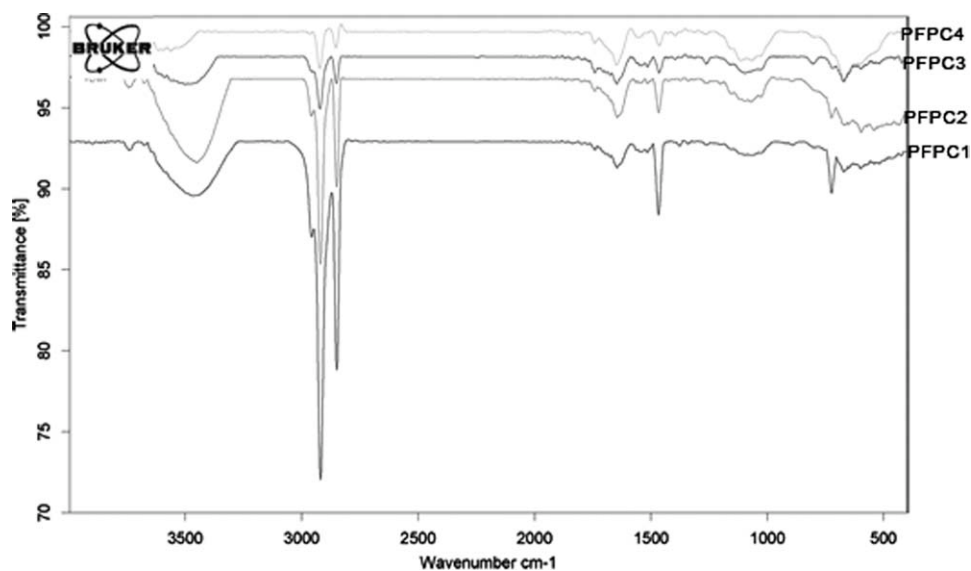


Figure 5 The FTIR spectra of PFPC1, PFPC2, PFPC3, and PFPC4.

under nitrogen. The nitrogen flow was 50 mL/min. Samples were measured in a platinum pan.

Differential scanning calorimetry (DSC) was performed in both nitrogen and oxygen atmospheres by means of DT-50 thermal analyzer from 20°C to 180°C for N₂ and 20°C to 600°C for air atmosphere, with a linear heating rate of 15°C/min, maintained at 200°C for 1 min to remove thermal history. The nitrogen flow rate was 30 mL/min. The precision of the calorimeter and temperature measurements were $\pm 2.0\%$ and $\pm 2.0^\circ\text{C}$, respectively. Samples were measured in an aluminum pan with a mass of about 10 mg under N₂ and platinum pan under air atmosphere. Thermal properties, melting temperature, and enthalpy of melting were determined from the DSC. The latent heat was calculated as the total area under the peaks of solid–solid and solid–liquid transitions of the paraffin and melting peaks of FPE in the composites by thermal analysis software.

TABLE II
FTIR Band Assignments of the PFPCs

Absorption peak (cm ⁻¹)	Band assignment
3761, 3696, 3622	Al–O–H
3440	Stretching vibration of O–H
2917	Asymmetric stretching vibration of C–H
2850	Symmetric stretching vibration of C–H
1741	Stretching vibration of C=O
1645	Distortion vibration of O–H
1468	CH ₂ or CH ₃ deformation vibration
1380	CH ₃ (end group)
1217	C–O stretching vibration
~1000	Al–OH stretching vibration
723	CH ₂ rocking vibration of (CH ₂) _n , n = 4

RESULTS AND DISCUSSION

Morphology and structure characterizations of composites

Scanning electron microscopy

The morphology of clean PE, hydrated alumina-FPE, Paraffin–alumina-Filled PE Composite PFPC1, and PFPC2 was investigated by SEM. The images of them are shown in Figures 1 and 2. The SEM images in Figures 1(c,d) and 2(c,d) also indicate that the hydrated alumina are well dispersed in net structure, and the alumina particles are embedded into the paraffin–alumina-FPE composites. SEM studies show that the paraffin is well dispersed in the three-dimensional net structure formed by the FPE, as indicated in Figure 2(a,b).

X-ray diffraction

The results obtained from X-ray diffraction spectra in all samples show the appropriate peaks of saturated and linear olefins ($d = 4.09 \text{ \AA}$). These peaks are more intense in the paraffin sample, making its high crystallinity and regular structure more obvious. In the FPE composites, new weak peaks were observed. These new peaks, suitable with Al- and O-containing

TABLE III
TGA Data of Samples

Samples	T_{onset}	$T_{-30 \text{ wt \%}}$	$T_{-70 \text{ wt \%}}$	Residue (580°C) %
Clean PE	~400	530	551	0.4
Filled PE	45	513	545	10.7
PFPC1	150	353	537	4
PFPC2	140	363	537	4

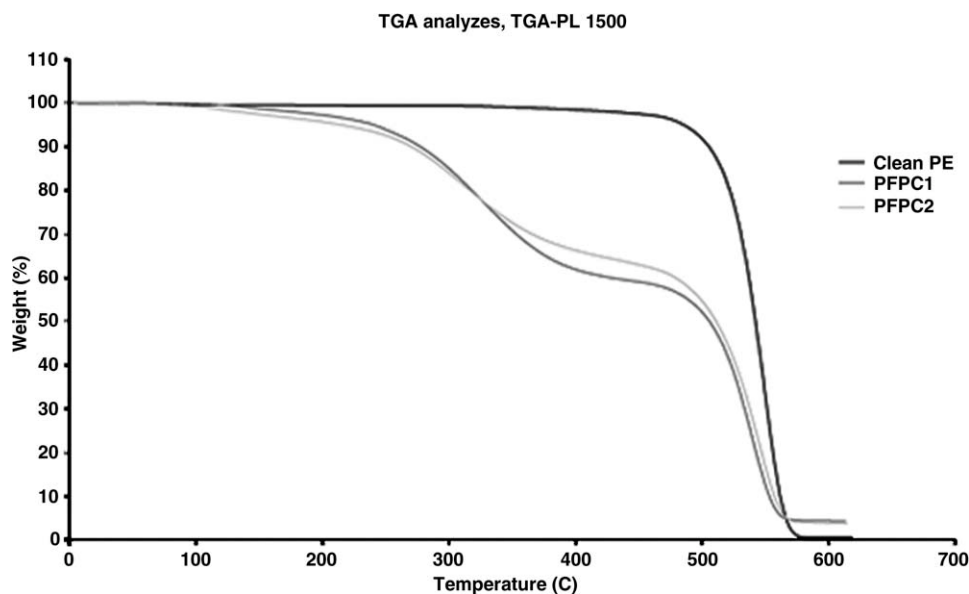


Figure 6 The TGA curves of clean PE, PFPC1, and PFPC2.

compounds, are compared with standard peaks of alumina and with various forms of hydrated alumina. The comparison shows that these peaks are more suitable for the monoclinic hydrated alumina and trigonal alumina structure (Fig. 3).

Fourier-transform infrared spectroscopy

Figures 4 and 5 display the FTIR spectra of composites. All of them have the characteristic bands: 2920, 2850, 1741, 1645, 1468, 1380, 1217, and 721 cm^{-1} . The assignments of the main peaks are listed in Table II. Besides these bands, the FPE has the characteristic bands of hydrated alumina. Sharp absorption peaks at 3761, 3696, 3622, and 3527 cm^{-1} correspond to large amount of hydroxyl groups of hydrated alumina (Al—O—H). The FPE and PFPCs also have the characteristic bands at 3440 and 1645 cm^{-1} corresponding to the stretching vibration and distortion vibration of the O—H group, respectively. This clearly indicates that many O—H groups are on the surface of alumina particles because of the intense absorption effect of them, and finally $\sim 1000 \text{ cm}^{-1}$ corresponding to the stretching vibration of Al—O of (hydrated) alumina.^{16,17}

Thermal properties of composites

Thermogravimetric analyses

The weight-loss data of the clean PE, hydrated alumina-FPE, PFPC1, and PFPC2 obtained from the TGA curves with respect to the temperature are shown in Table III. The TGA curves are shown in Figure 6. It can be seen from the TGA curves that there are two-step degradation processes in the PFPC1 and PFPC2. The first step of degradation occurs about from 200°C to 450°C, corresponding to the degradation of the paraffin molecular chain. The second step happens from about 450–600°C. This step may be assigned to the degradation of the PE main chains.

The results show that the thermal stability of the composites decreases with an increase in paraffin content as a consequence of the lower thermal stability of the paraffin. The lower onset temperature and 15% weight loss temperature for hydrated alumina-FPE was due to the loss of water. $\text{Al}(\text{OH})_3$ is known to decompose endothermically on heating and produces H_2O and Al_2O_3 . Because of the endothermic nature of the reaction, metal hydroxide should absorb the heat from the polymer and should delay the thermal

TABLE IV
The Parameters of Paraffin-Filled PE Composites Obtained from DSC Measurements

Sample	Phase transition, T_p (°C)	Phase change, T_p (°C)	Alumina-filled PE, T_p (°C)	$\Delta H_m(\text{Pa})$ (J/g)		Theo. $\Delta H_m(\text{FPE})$ (J/g)	$\sum \Delta H_m(\text{Th})$ (J/g)	$\sum \Delta H_m(\text{Ex})$ (J/g)
				Theo.	Exp			
Paraffin	43.4	63	—	—	227.7	—	—	227.7
FPE	—	—	145.6	—	—	—	—	160
PFPC1	43.4	63.7	136	68.3	55.8	112	180.3	193.7
PFPC2	46.9	64.6	140.5	45.5	28.8	128	173.5	174
PFPC3	Not visible	63	145.1	22.8	11	144	166.8	167.1
PFPC4	Not visible	62.6	143.5	11.4	6.8	152	163.4	162.3

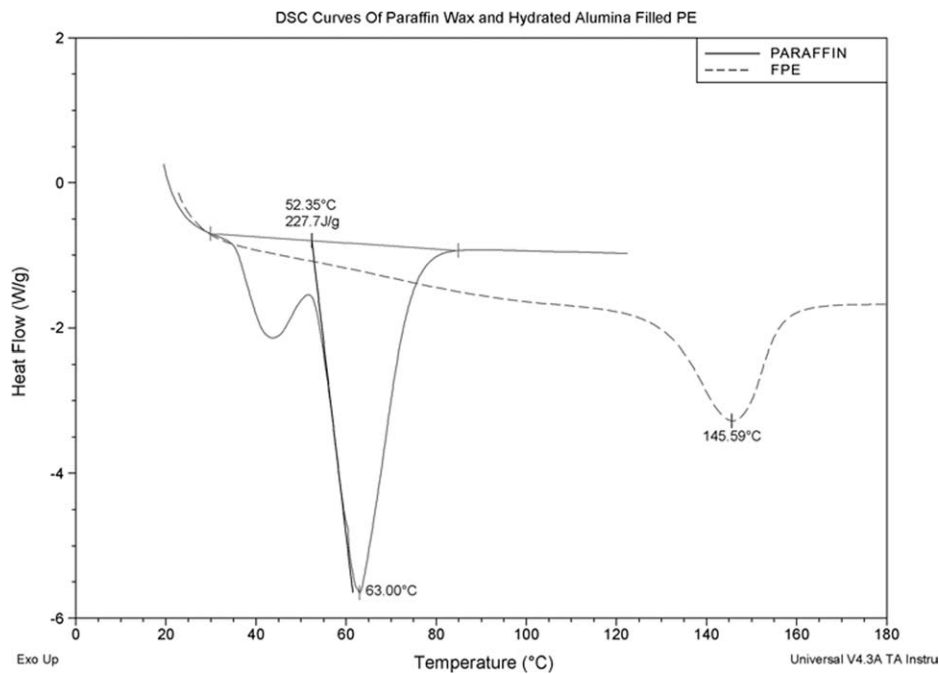


Figure 7 The DSC curves of pure paraffin and hydrated alumina-FPE.

degradation. The appearance of excessive weight loss might be due to the excessive loss of water rather than decomposition of the polymer itself.¹⁸

Differential scanning calorimetry

Under N₂ atmospheres. The results obtained from DSC analyses of paraffin, FPE, and their composites are summarized in Table IV. The DSC curves for

pure paraffin and FPE are shown in Figure 7, and those of their composites are shown in Figure 8. The DSC curve of pure paraffin displays two well-defined separated peaks at 43.4°C and 63°C, which are clearly distinguishable from each other, thus indicating a mixture of several molecular sizes. The first peak relates to the solid–solid transition of the paraffin and the second main peak is associated with the solid–liquid phase change of the paraffin.

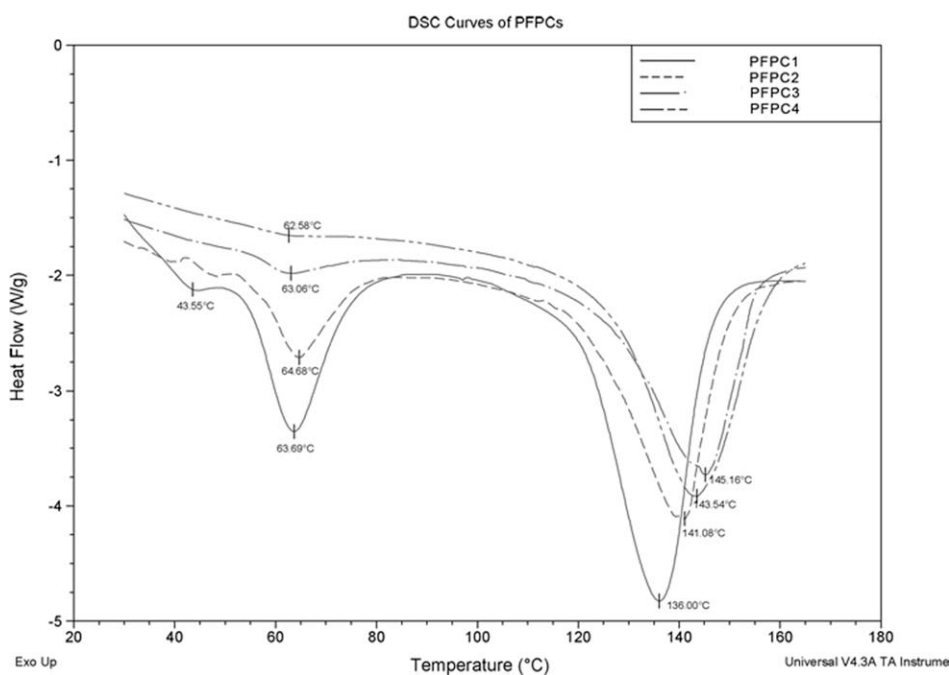


Figure 8 The DSC curves of paraffin and alumina-FPE composites (PFPCs).

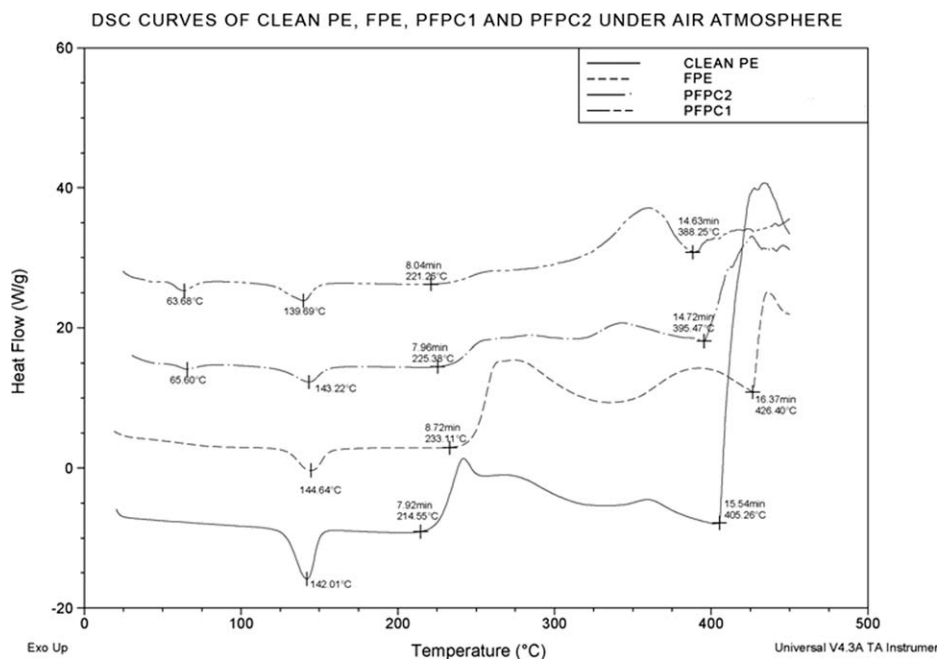


Figure 9 The DSC curves of pure PE, hydrated alumina-FPE, PFPC1, and PFPC2 under air atmospheres.

Peak of the melting temperature of FPE was found to be 145.6°C. Figure 7 shows that the phase change peaks of the paraffin are still in existence in the composites because the paraffin is a homologous compound of PE, and there is no chemical reaction among the paraffin and PE during the preparation of the composites. However, the phase change peaks of the paraffin are weaker than those of the pure paraffin.^{2-4,7,11} In the PFPCs, the melting temperature of PE decreases with an increase in paraffin content, which indicates the formation of smaller crystallites because of the miscibility of the components in the molten state. The total specific enthalpy of melting was evaluated by the use of a linear baseline over a broad thermal interval (30–165°C for all samples). The melting latent heat of all the blends increases with an increase in paraffin content, which is the result of the higher crystallinity of the paraffin. This increase is in excellent agreement with the additive rule, given by eq. (1):

$$\sum \Delta H_m(\text{Th}) = w_{\text{pa}} \Delta H_m(\text{Pa}) + w_{\text{FPE}} \Delta H_m(\text{FPE}) \quad (1)$$

where $\Delta H_m(\text{Th})$ is the total theoretically calculated melting enthalpy, $\Delta H_m(\text{FPE})$ and $\Delta H_m(\text{Pa})$ are the

melting enthalpies for alumina-FPE and paraffin wax, respectively, and w_{FPE} and w_{pa} are their weight portions, respectively. This indicates that the concentration of paraffin in the blends corresponds to the theoretically calculated portion. This is an important conclusion because it confirms that there is no leakage of paraffin from the blends during the sample preparation (mixing and compression molding).¹¹

As indicated in Table IV, transition temperature and paraffin melting temperature values for all of the composites approach those of the pure paraffin. However, the latent heat values of the paraffin decrease markedly compared with the pure paraffin. For example, the partial latent heat between 25°C and 70°C of PFPC1 should be 68.3 J/g by multiplying the latent heat of the dispersed paraffin (227.7 J/g) with its mass fractions (30 wt %). It may be that the three-dimensional net structure confines the molecule's movement of paraffin in form-stable PCM and the paraffin partially intercalates the interlayer of the hydrated alumina, but the total experimental latent heat of composites is approximately equal with the total theoretical calculations. Although the latent heat of the composites has a certain degree of decrease, their thermal stability has marked enhancements.

TABLE V
The Parameters of Pure PE, FPE, and Their Composites Obtained from DSC Measurements under Air Atmosphere

Sample	PE, T_p (°C)	Exp $\sum \Delta H_m(\text{Ex})$ (J/g)	Oxidation temp. (°C)		Oxidation time (min)	
			First peak start	Major peak start	First peak start	Major peak start
PE	141.9	312	214.5	405.3	7.98	15.54
FPE	144.6	272	233.1	426.4	8.72	16.37
PFPC1	139.6	318	221.3	388.3	8.04	14.63
PFPC2	143.2	314	225.4	395	7.96	14.72

Under air atmospheres. Thermal oxidation behavior of the clean PE, hydrated alumina-FPE, PFPC1, and PFPC2, under air atmosphere conditions in the median temperature of 15–550°C was studied. The related DSC curves are shown in Figure 9. The results obtained from DSC analyses of clean PE, FPE, PFPC1, and PFPC2 are summarized in Table V. As the curve is also specified, the process of thermal destruction of hydrated alumina-FPE occurs later than clean PE at higher temperatures. In other words, the curve shifts to the right. A comparison of the thermal oxidation curve of pure PE and FPE shows delay in thermal oxidation and destruction of FPE; thus, the first exothermal peak of pure PE indicates that beginning of polymer thermal oxidation occurs at the temperature of 214°C, whereas this operation for the alumina FPE occurs at the temperature of 233°C. It is known that the combination of paraffin in the PE reduces the melting temperature and thermal oxidation, but in the presence of alumina, the thermal oxidation occurs in higher temperatures than that in pure PE.

The following arrangement shows the increase in oxidation temperature of four samples:

$$FPE > PFPC2 > PFPC1 > PE.$$

It can be simply stated that the thermal oxidation leads to the destruction of the polymer structure and the phenomena of the combustion are directly related. The oxidation time that leads to destruction of PE occurs later, in the same amount the combustion of composites will happen later.

CONCLUSIONS

PCMs based on paraffin–alumina-FPE composites with improved thermo-oxidation stability properties were successfully prepared. The SEM images showed that the alumina-FPE acted as the supporting material and formed the three-dimensional net structure. The paraffin acted as a PCM and dispersed in the network structure. The alumina particles dispersed in the matrix and did not show notable agglomerations. The FTIR spectra contained the characteristic band of aluminum oxide at $\sim 1000\text{ cm}^{-1}$, which corresponds to the stretching vibration of Al-O bending vibration of alumina. In addition,

the absorption peaks at 3440 and 1645 cm^{-1} correspond to the stretching vibration and distortion vibration of the hydroxyl (O-H) group, respectively. The intense absorption indicates that there are many O-H groups on the surface of the alumina nanoparticles. It was also seen from the TGA curves that there are two-step degradation processes in the PFPCs. The first step of degradation corresponds to the degradation of the paraffin molecular chain, and the second step corresponds to the degradation of the PE main chains. Lastly, the DSC measurements revealed that the alumina particles had little effect on the thermal energy storage but improved the thermo-oxidation properties of the composites.

References

1. Stritih, U. *Energy Buildings* 2003, 35, 1097.
2. Hong, Y.; Xin-Shi, G. *Solar Energy Mater Solar Cells* 2000, 64, 37.
3. Sari, A. *Energy Conversion Manage* 2004, 45, 2033.
4. Cai, Y.; Song, L.; He, Q.; Yang, D.; Hu, Y. *Energy Conversion Manage* 2008, 49, 2055.
5. Zhang, Y.; Ding, J.; Wang, X.; Yang, R.; Lin, K. *Solar Energy Mater Solar Cells* 2006, 90, 1692.
6. Sharma, A.; Tyagi, V. V.; Chen, C. R.; Buddhi, D. *Renew Sustain Energy Rev* 2009, 13, 318.
7. Chen, C.; Wang, L.; Huang, Y. *Solar Energy Mater Solar Cells* 2008, 92, 1382.
8. Xiao, M.; Feng, B.; Gong, K. *Solar Energy Mater Solar Cells* 2001, 69, 293.
9. Hasnain, S. M. *Energy Conversion Manage* 1998, 39, 1127.
10. Peng, S.; Fuchs, A. *J Appl Polym Sci* 2004, 93, 1240.
11. Krupa, I.; Mikova, G.; Luyt, A. S. *Eur Polym J* 2007, 43, 4695.
12. Xiao, M.; Feng, B.; Gong, K. C. *Energy Conversion Manage* 2002, 43, 103.
13. Yibing, C. A. I.; Wei, Q.; Huang, F.; Weidong, G. A. O. *Appl Energy* 2008, 85, 765.
14. Kaminsky, W. *Metal Organic Catalysts for Synthesis and Polymerization: Recent Results by Ziegler-Natta and Metallocene Investigations*. Springer: New York, 1999; p 674.
15. Azizov, A. G.; Aliyeva, R. V.; Martynova, G. S.; Bagirova, Sh. R.; Kalbalieva, E. S. Polymerization of ethylene in the presence of novel single-site titanium phenolate catalytic systems. *Russian in Vysokomolekulyarnye Soedineniya, Ser. B*, 2009, Vol. 51, pp. 2152–2159.
16. Jin, B.; Zhang, W.; Sun, G.; Gu, H.-B. *J Ceram Process Res* 2007, 8, 336.
17. Lee, H. W.; Park, B. K.; Tian, M. Y.; Lee, J. M. *J Ind Eng Chem* 2006, 12, 295.
18. Murty, M. V. S.; Grulke, E. A.; Bhattacharyya, D. *Polym Degrad Stab* 1998, 61, 421.